N-(naphthyl)-N'-(methoxy carbonyl)thiocarbamide and its Cu(I) complex: synthesis, spectroscopic, X-ray, DFT and in vitro cytotoxicity study

Durga P. Singh, Seema Pratap, Sunil K. Pandey, Ray J. Butcher & Gaetano Marverti

View supplementary material

Accepted author version posted online: 27 Oct 2014.
Published online: 19 Nov 2014.

Submit your article to this journal

Article views: 93

View related articles

View Crossmark data

Taylor & Francis
Taylor & Francis Group

N-(naphthyl)-N′-(methoxy carbonyl)thiocarbamide and its Cu (I) complex: synthesis, spectroscopic, X-ray, DFT and *in vitro* cytotoxicity study
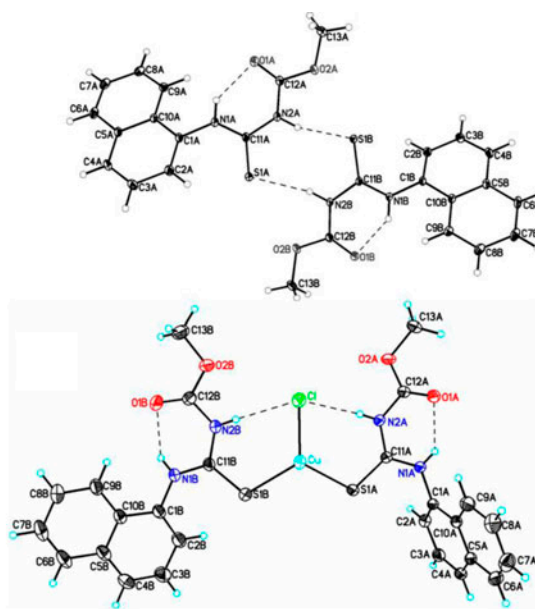
DURGA P. SINGH†, SEEMA PRATAP*†, SUNIL K. PANDEY†, RAY J. BUTCHER‡
and GAETANO MARVERTI§

†Department of Chemistry (M.M.V), Banaras Hindu University, Varanasi, India
‡Department of Chemistry, Howard University, Washington, DC, USA
§Department of Biomedical Sciences, Metabolic and Neurosciences, University of Modena at Reggio
Emilia, Modena, Italy

The structural characterization of two new compounds N-naphthyl-N′-methoxycarbonyl thiocarbam-ide (NMCT) (**1**) and its Cu(I) complex, bis(N-naphthyl-N′-methoxycarbonyl thiocarbamide) copper (I) chloride [(NMCT)₂CuCl] (**1a**) have been done by spectroscopic techniques (FT-IR, ¹H NMR, ¹³C NMR and electronic spectroscopy) and X-ray crystallography. To get a deeper insight of vibra-tional frequencies and electronic transitions, DFT and TD-DFT studies have also been performed. X-ray study revealed trigonal planar geometry around copper(I). The ligand coordinates through thi-one sulfur only. The cytotoxicity of **1** and **1a** has been assayed in five human carcinoma cell lines,

---

*Corresponding author. Email: drseemapratap@gmail.com

2008, C13* (cervical carcinoma), A2780, A2780/CP and IGROV-1 (ovarian carcinoma). Both the compounds exhibited cytotoxicity. The inhibitory activity of copper complex was better than ligand against all the cell lines.

1. Introduction

Transition metal complexes have been tested for their antitumor activities to find an effective and safe drug for the treatment of cancer. Many copper complexes with N,N-disubstituted thiourea ligands have shown promising inhibitory activity against various human cancer cell lines [1–6]. Cytotoxic properties of the complexes are affected considerably by structural changes in the ligand framework [4, 6]. Copper is an essential trace metal and has been used for many years either as copper ions or in complexes to disinfect liquids, solids, and human tissues [7]. The coordination behavior and therapeutic potential of N,N-disubstituted thioureas having N, O, and S as donor atoms have been widely reported. Two commonly encountered coordination modes are (1) coordination through thione sulfur and (2) coordination through oxygen and sulfur [8–15]. The third, very rare, is coordination through N and S forming a four-membered chelate ring with the metal ions [16–19]. The pharmacological importance of the transition metal complexes of substituted thioureas is evident by their use as antiviral, antibacterial, antifungal, antitubercular, antithyroidal, insecticidal, antimalarial agents, etc. [20–26]. These complexes also find applications in liquid–liquid extraction, as catalysts in oxidation reactions and as cation and anion sensors [27–31]. The anticancer properties of N,N′-substituted thioureas and their complexes have not been explored much despite appreciable activity displayed by some. The above facts encouraged us to pursue this work.

To understand and analyze the spectral properties of the ligand and complex, we have carried out DFT calculations on both using B3LYP functional. DFT coupled with TD-DFT calculations have been performed to ascertain the nature of orbitals involved in transition processes and to correlate the structural parameters with the spectroscopic properties of the complex [32–36].

2. Experimental

2.1. *Materials and instrumentation*

Copper(II) chloride, methyl chloroformate, naphthylamine, and ammonium thiocyanate were purchased from Merck chemicals. Acetone, chloroform, and dichloromethane were purchased from Rankem. Elemental analyses were performed on a CE-440 Exeter Analytical CHN analyzer. Infrared spectra of the title compounds as KBr pellets (4000–400 cm^{-1}) were recorded on a Varian 3100 FT-IR Excalibur series spectrophotometer. ^{1}H and ^{13}C NMR spectra were obtained on a JEOL FT-NMR AL 300 spectrometer in CDCl$_3$ with chemical shifts relative to SiMe$_4$. Electronic spectra were recorded on an (UV)-1700 Pharma Spec. Shimadzu UV–visible spectrophotometer. Room temperature magnetic susceptibility measurements were performed on a Cahn Faraday balance using Co[Hg (SCN)4] as standard. The magnetic susceptibility was corrected for diamagnetism using Pascal's constants [37].

2.2. *Synthesis*

2.2.1. Synthesis of N-naphthyl-N′-methoxycarbonylthiocarbamide (NMCT) (1). The ligand is synthesized by a slight modification in the reported method [38]. A solution of methyl chloroformate in acetone (30 cm^3) was added dropwise to the solution of ammonium thiocyanate (0.76 g, 10 mM) in acetone (30 cm^3) for 10 min. The resulting solution was refluxed for 45 min. After cooling to room temperature, a solution of naphthylamine (1.431 g, 10 mM) in acetone (30 cm^3) was added dropwise to the above solution and the resulting mixture was further refluxed for 90 min. The precipitated ammonium chloride was filtered off and the yellowish clear solution was evaporated in vacuum to dryness to get a crude yellowish brown product. Single crystals suitable for X-ray diffraction were obtained by slow evaporation of acetone solvent in two weeks.

Yield: 76%, m.p.; 198–200 °C. Elemental analyses: calculated for $C_{13}H_{12}N_2O_2S$ (%), C, 59.98; H, 4.64; N, 10.76; Found, C, 59.91; H, 4.60; N, 10.70. IR (KBr, cm^{-1}): 3435(br) ν_{as}(N–H), 3151(m) ν_s(N–H), 3009 (aromatic C–H), 2960 (aliphatic C–H), 1725 (–COOMe), 1546 (Ar, C=C), 1534 (vs) δ(N–H), 1347, ν(N=C=N); 1245, ν(N–C–S); 1204, ν(C–N); [–N–C(S)–N], 1034, 774, 722(w) δ(Ar C–H); ^{1}H NMR (300 MHz, CDCl$_3$, 25 °C): δ 11.20 (s, –CSN<u>H</u>), 8.37 (s, 1H, –CON<u>H</u>), 7.46–7.19 (m, 7H, C$_{10}$H$_7$), 3.89 (s, 3H, –COOC<u>H</u>$_3$); ^{13}C NMR (75 MHz, DMSO, 25 °C): 180.42 (C, <u>C</u>=S), 154.30 (C, –<u>C</u>OOMe), 134.26, 133.69, 128.92, 128.29, 127.29, 126.63, 126.25, 125.41, 124.94, 122.14 (C, Aromatic), 53.09 (C, –COO<u>C</u>H$_3$).

2.2.2. Synthesis of bis[N-(naphthyl)-N′-(methoxycarbonyl) thiocarbamide]copper(I) chloride [(NMCT)$_2$CuCl] (1a). To 30 cm^3 ethanol solution of NMCT (**1**) (0.520 g, 2 mM), an ethanol solution of cupric chloride (0.172 g, 1 mM) was added with constant stirring. The stirring was continued at room temperature for 2 h. The complex precipitated as green solid, was filtered, washed with ethanol, and dried in vacuum. Single crystals suitable for X-ray diffraction were obtained after one week by slow evaporation of dichloromethane–ethanol (1 : 2, v/v) solution of the complex.

Yield: 68%, m.p.; decompose at 218–221 °C. Elemental analyses: calculated for $C_{26}H_{24}CuN_4O_4S_2CuCl$ (%), C, 45.71; H, 3.54; N, 8.20; Found, C, 45.78; H, 3.59; N, 8.26. IR (KBr, cm^{-1}): 3169(w) ν(N–H), 3103(m) ν(aromatic C–H), 2961 (aliphatic C–H), 1746 (s) (–<u>C</u>OOMe), 1549 (Ar, C=C), 1525(vs) δ(N–H), 1368(m) ν(NCN), 1230(m) ν(C=S) [–C(S)–NH], 1226 ν(C–N) [–C(O)–NH], 1178 ν(C–N + C–S) [–N–C(S)–N], 729(w) δ(Ar C–H). ^{1}H NMR (300 MHz, CDCl$_3$, 25 °C): δ 11.68 (s, 2H, –CSN<u>H</u>), 11.33 (s, 2H, –CON<u>H</u>), 7.86–7.45 (m, 14H, C$_{20}$H$_{14}$), 3.80 (s, 6H, –COOC<u>H</u>$_3$); ^{13}C NMR (75 MHz, DMSO, 25 °C): 179.57 (C, <u>C</u>=S), 153.44 (C, –<u>C</u>OOMe), 133.61, 133.33, 128.54, 127.93, 127.41, 126.40, 126.01, 125.10, 124.78, 121.90 (C, Aromatic), 52.91 (C, –COO<u>C</u>H$_3$).

2.3. *Crystal structure determination*

Crystal data for **1** was collected using CrysAlisPRO on an OXFORD DIFFRACTION XCALIBER Super Nova, Dual, Cu at zero, Atlas' diffractometer using graphite-monochromated Mo *Kα* radiation (λ = 0.71073 Å) at 100 K, whereas data collection for **1a** was performed using a CrysAlisPRO on an OXFORD DIFFRACTION XCALIBER Ruby Gemini CCD diffractometer using graphite monochromated Mo Kα (λ = 0.71073 Å) at 123 K. The unit cell parameters were obtained from 39,896 and 15,713 reflections in the cell

Table 1. Summary of crystallographic data and structural parameters of NMCT (**1**) and [(NMCT)$_2$CuCl] (**1a**).

Compound	NMCT (**1**)	[(NMCT)$_2$CuCl] (**1a**)
Empirical formula	$C_{13}H_{12}N_2O_2S_1$	$C_{26}H_{24}ClCuN_4O_4S_2$
Formula weight	260.06	619.6
T (K)	100(2)	123(2)
λ (Å)	0.71073	0.71073
Crystal system	Triclinic	Triclinic
Space group	P-1	P-1
a (Å)	10.979(5)	9.1737(5)
b (Å)	11.143(5)	11.0979(7)
c (Å)	11.531(5)	14.6139(8)
α (°)	88.635(5)	75.599(5)
β (°)	79.402(5)	75.546(5)
γ (°)	62.252(5)	70.611(5)
V (Å^3)	1224.1(9)	1336.43(13)
Z	4	2
D_{Calcd} (g cm^{-3})	1.412	1.54
μ (cm^{-1})	0.259	1.114
R $(F_o{}^2)^a$	0.0483	0.0496
Rw $(F_o{}^2)^b$	0.1342	0.101
GooF	1.044	1.026

$^aR = P\|F_o| - |F_c\|/\sum|F_o|$.
$^bR_w = [\sum w(F_o{}^2 - F_c{}^2)^2/\sum w(F_o{}^4)]^{1/2}$.

measurement angle range 2.641–41.281° and 3.22–32.64° for **1** and **1a**, respectively. The structures were solved by direct methods and refined by full matrix least squares on F^2 using SHELX-97 [39]. The non-hydrogen atoms were refined with anisotropic thermal parameters. All hydrogens were geometrically fixed and allowed to refine using a riding model. The refinement converged to a final $R_1 = 0.0558$, $wR_2 = 0.1675$ for **1** and $R_1 = 0.0446$, $wR_2 = 0.0867$ for **1a**. Important crystal data are presented in table 1 and selected interatomic distances and angles in table 2. Drawings were made using ORTEP-III [40] and Mercury [41].

2.4. Computational details

The molecular structures of **1** and **1a** were optimized using density functional theory (DFT) with the GAUSSIAN-03 program package [42] employing the B3LYP (Becke three parameter Lee-Yang-Parr exchange correlation functional), which combines the hybrid-exchange functional of Becke [43] with the gradient-correlation functional of Lee, Yang and Parr [44] and the 6-311 + G(d,p) basis set [45]. Starting geometries were taken from X-ray refinement data. The harmonic vibrational frequencies were calculated at the same level of theory for the optimized structure. Absence of any imaginary vibrational frequencies indicates that the geometries were at the minimum of the potential surface. Electronic spectra were also predicted at the same level of theory and basis set.

2.5. Biological assays

2.5.1. Cell lines. Two human cervical cancer cell lines (2008 and C13*) and three ovarian cancer cell lines (IGROV-1, A2780, and A2780/CP) were used. Among these, C13* and A2780/CP are cisplatin (ccDDP)-resistant cells [46, 47]. Cells were grown as monolayers in RPMI 1640 medium containing 10% heat-inactivated fetal bovine serum and 50 μg mL^{-1}

Table 2. Selected bond lengths (Å), bond angles (°), and hydrogen bonding interactions for NMCT (**1**) and [(NMCT)$_2$CuCl] (**1a**) obtained from X-ray diffraction and DFT calculation.

NMCT (**1**)	Molecule A	Molecule B	DFT calc.	[(NMCT)$_2$CuCl] (**1a**)	Mol. A	Mol. B	DFT calc. A	Mol. B
Point group			C1	Point group			C1	
Energy (Hartree)			1161.13	Energy			4422.91	
Dipole moment (D)			3.799	Dipole moment			0.8316	
Bond lengths (Å)				Bond lengths (Å)				
S(1)–C(11)	1.6706(12)	1.6728(12)	1.668	Cu–Cl	2.245		2.29	
N(2)–C(11)	1.3837(11)	1.3833(11)	1.407	Cu–S(1)	2.2135	2.2402	2.28	2.28
N(1)–C(11)	1.3347(12)	1.3322(11)	1.349	S(1)–C(11)	1.6981	1.6948	1.702	1.702
N(1)–C(1)	1.4227(12)	1.4197(12	1.422	O(1)–C(12)	1.204	1.207	1.21	1.219
N(2)–C(12)	1.3755(13)	1.3764(13)	1.375	O(2)–C(12)	1.32	1.326	1.32	1.331
O(2)–C(12)	1.3301(12)	1.3291(11)	1.342	O(2)–C(13)	1.491	1.491	1.44	1.44
O(1)–C(12)	1.2122(12)	1.2148(12)	1.217	N(1)–C(11)	1.325	1.336	1.341	1.341
				N(2)–C(11)	1.362	1.428	1.379	1.43
				N(1)–C(1)	1.433	1.368	1.43	1.379
				N(2)–C(12)	1.387	1.377	1.38	1.383
Bond angles (°)								
				Bond angles (°)				
C(12)–N(2)–C(11)	126.95(7)	126.82(7)	129.25	S(1A)–Cu–S(1B)	119.46		120.04	
C(11)–N(1)–C(1)	125.63(8)	126.96(8)	128.04	S(1A)–Cu–Cl	121.22	119.29	119.97	119.97
N(1)–C(11)–N(2)	116.17(8)	116.27(8)	114.37	C(11A)–S(1A)–Cu	109.54	110.05	110.14	110.26
N(1)–C(11)–S(1)	125.05(7)	125.65(7)	128.22	C(11A)–N(1A)–C(1A)	125.35	129.67	125.56	126.78
N(2)–C(11)–S(1)	118.77(6)	118.07(6)	117.4	C(11A)–N(2A)–C(12A)	125.97	127.39	126.59	126.67
O(1)–C(12)–O(2)	125.05(9)	125.38(8)	124.43	C(2A)–C(1A)–N(1A)	119.63	122.42	119.64	126.27
O(1)–C(12)–N(2)	125.67(8)	125.61(8)	125.34	C(10A)–C(1A)–N(1A)	118.54	116.56	119.17	118.57
O(2)–C(12)–N(2)	109.27(8)	109.00(7)	109.62	N(1A)–C(11A)–N(2A)	117.61	116.66	116.95	116.68
				N(1A)–C(11A)–S(1A)	121.1	124.31	121.92	122.48
				N(2A)–C(11A)–S(1A)	121.29	119.03	121.13	1120.85
				O(1A)–C(12A)–N(2A)	124.76	125.43	125.69	125.69

Important hydrogen bonding interaction for **1** [Å and °]				
	D–H	D···A	H···A	<(DHA)
N(1A)–H(1AA)···O(1A)	0.88	2.6627(13)	1.96	135.7
N(2A)–H(2AB)···S(1B)#1	0.88	3.2844(14)	2.44	161.9
C(13A)–H(13C)···O(1B)#2	0.98	3.5323(19)	2.57	168.4
N(1B)–H(1BA)···O(1B)	0.88	2.6646(13)	1.96	136.5
N(2B)–H(2BB)···S(1A)#3			2.52	155.6
C(13B)–H(13E)···O(1A)#4			2.64	148.9

Important hydrogen bonding interaction for **1a** [Å and °]				
	D–H	D···A	H···A	<(DHA)
N(1A)–H(1A)···O(1A)	0.80(2)	2.634(2)	2.01(2)	134(2)
N(2A)–H(2A)···Cl	0.78(2)	3.2145(15)	2.43(2)	173.2(19)
N(1B)–H(1B)···O(1B)	0.80(2)	2.667(2)	1.99(2)	142(2)
N(2B)–H(2B)···Cl	0.785(19)	3.2126(16)	2.431(19)	174.3(18)

Note: Symmetry transformations used to generate equivalent atoms: #1 $x + 1$, y, $z − 1$; #2 x, y, $z − 1$; #3 $x − 1$, y, $z + 1$; #4 x, y, $z + 1$.

gentamycin sulfate. All cell media and serum were purchased from Lonza (Verviers, Belgium). Cultures were equilibrated with humidified 5% CO_2 in air at 37 °C. All studies were performed in *Mycoplasma* negative cells, as routinely determined with the Myco Alert Mycoplasma detection kit (Lonza, Walkersville, MD, USA).

2.5.2. Cytotoxicity screening. Cytotoxicities of compounds used in the present study were determined by MTT assay [48]. The cells were seeded into 96-well plates and cultured overnight. Various concentrations of the test compounds dissolved in DMSO were then added and incubated for 72 h. After incubation, the medium was removed and 100 μL fresh culture medium was added containing 0.5 mg mL^{-1} MTT (3-(4,5-dimethylthiazol-2-yl)-2,5-diphenyl tetrazolium bromide; Sigma) and then incubated at 37 °C for 4 h. The medium was removed and 100 μL DMSO was added to dissolve the dark blue crystals. After incubation for 30 min at room temperature, to ensure that all crystals were dissolved, absorbance was measured using an ELISA plate reader at 570 nm with a reference wavelength of 650 nm.

3. Results and discussion

3.1. *Synthesis*

NMCT (**1**) was obtained by reacting methoxycarbonyl isothiocyanate and naphthylamine in acetone in 1 : 1 ratio as light brown crystalline solid, which on reacting with copper chloride in ethanol in 2 : 1 molar ratio, yielded light yellow [(NMCT)$_2$CuCl] (**1a**) (scheme 1).
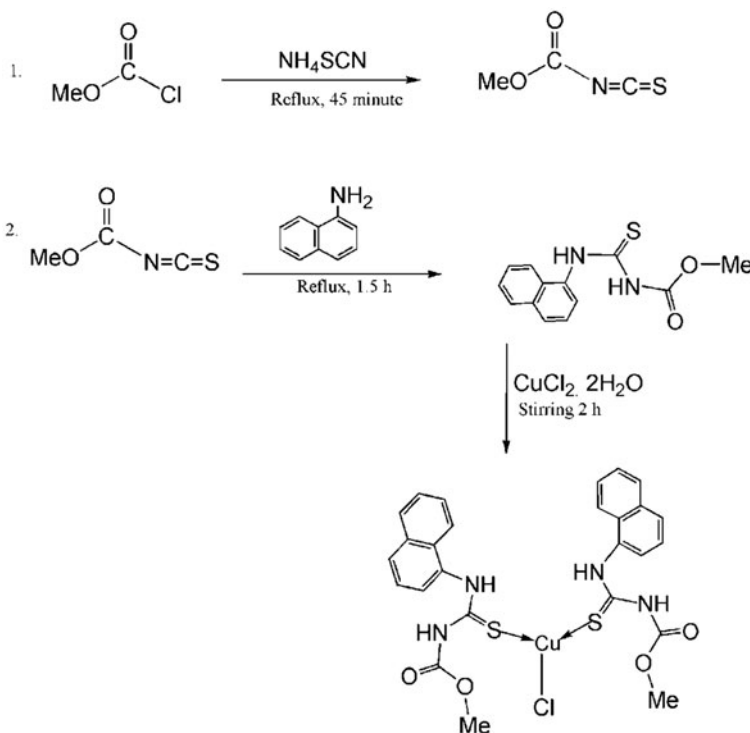
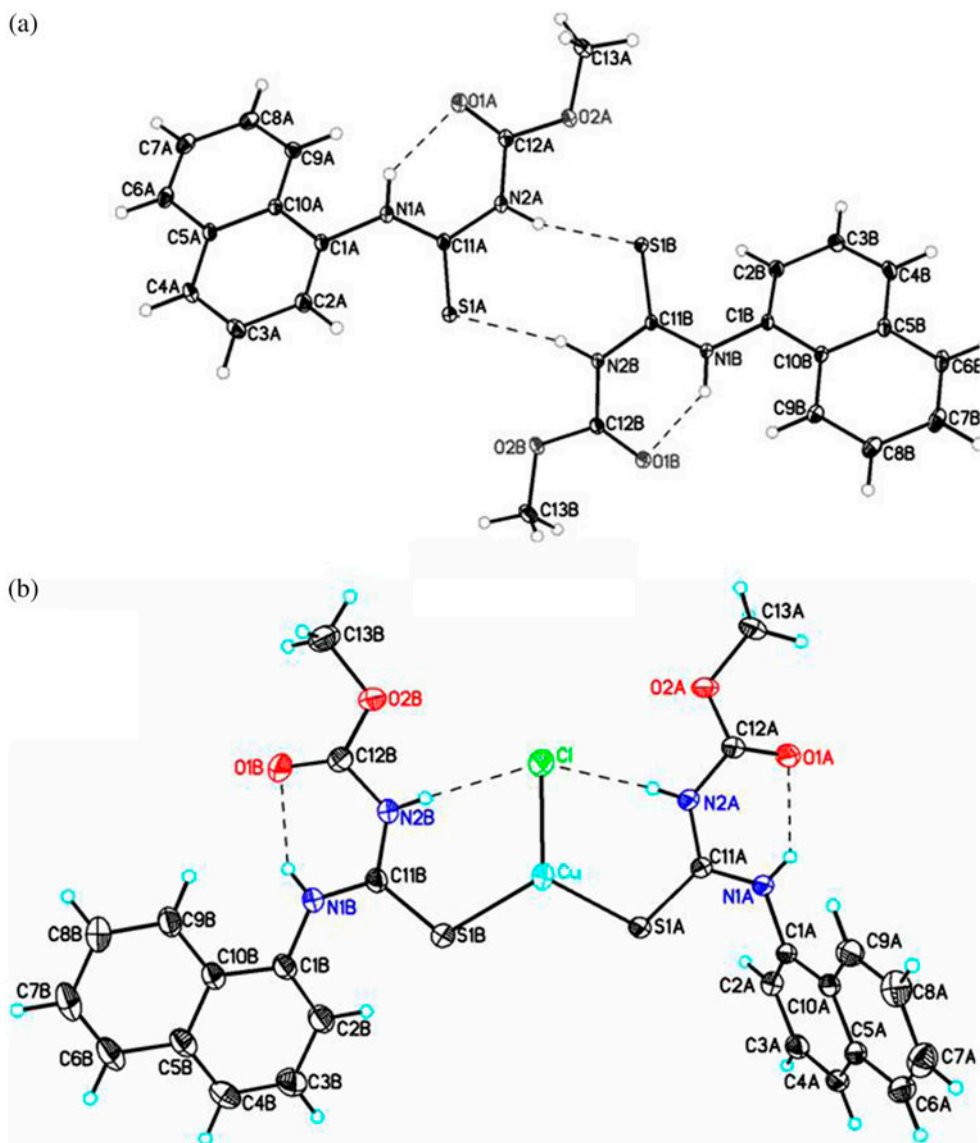Scheme 1.   Synthesis of N-(naphthyl)-N′-(methoxy carbonyl) thiocarbamide and its Cu(I) complex.

Figure 1. ORTEP view of (a) NMCT (**1**) and (b) [(NMCT)₂CuCl] (**1a**) showing atom labeling. Thermal ellipsoids are drawn at 50% probability level.

3.2. *Crystal structure descriptions*

The crystal structure, unit cell diagram, and packing pattern of NMCT (**1**) and [(NMCT)₂CuCl] (**1a**) are shown in figures 1(a) and (b), S1 (see online supplemental material at http://dx.doi.org/10.1080/00958972.2014.979165), and 2(a) and (b), respectively. The important crystallographic data, bond lengths, bond angles, and hydrogen bonds for both the compounds together with DFT-calculated values are presented in tables 1 and 2. The *trans* orientation of the carbonyl and thiocarbonyl moieties across the C–N bond remains intact in the crystal structure of complex due to the non-involvement of carbonyl in
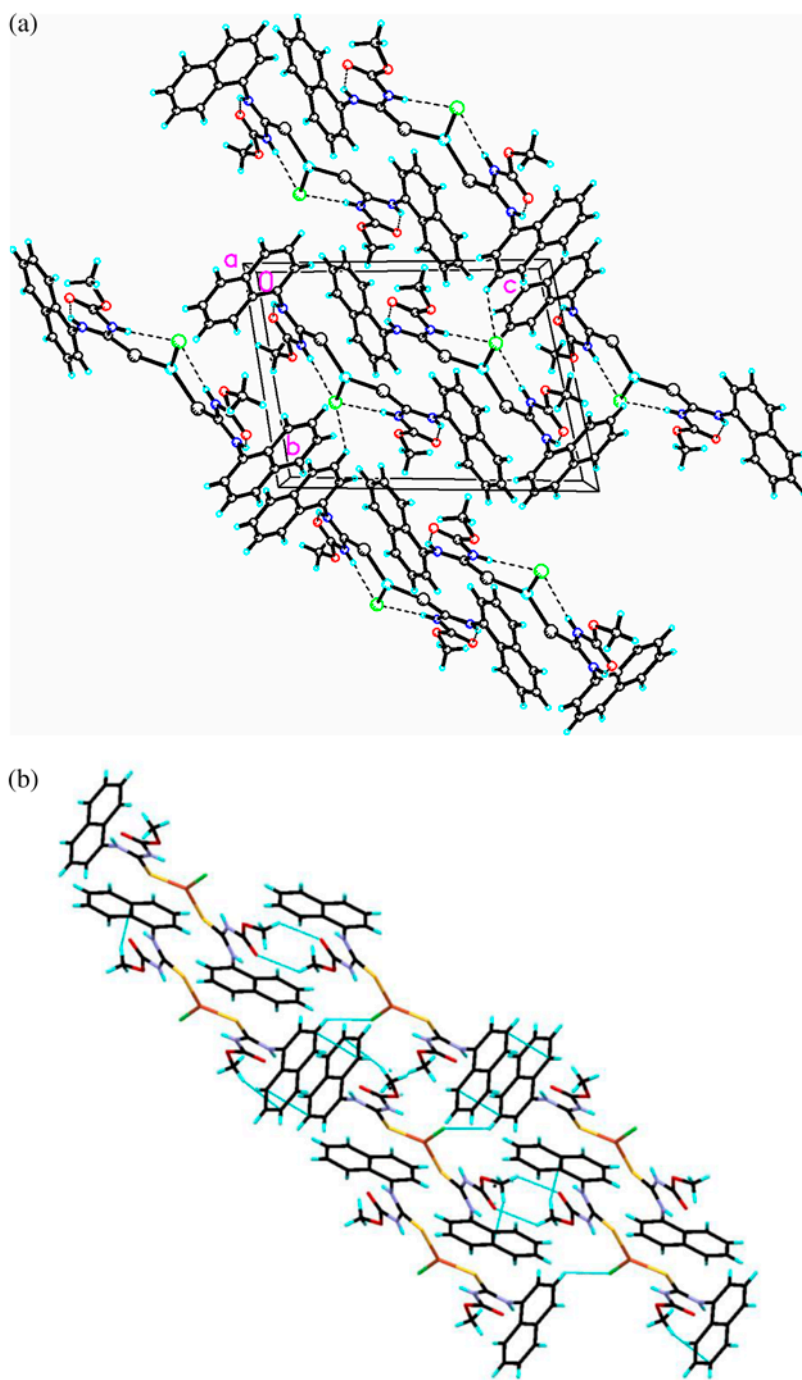
Figure 2. (a) Unit cell diagram of **1a**. (b) Weak intermolecular interactions (C–H···O, C–H···Cl, Cπ···Cπ) stabilize the crystal packing and lead to infinite chain length along the *c*-axis.

coordination. In ligand structure, the slightly twisted position of naphthyl ring with respect to the plane of the molecule is evident by the dihedral angles [53.40(0.07)° and 46.21(0.17)°] formed between thiourea fragment (N1/C11/S1/N2) and naphthyl ring (C1/C2/C/C4/C5/C6/C7/C8/C9/C10) and between the mean plane of naphthyl ring and methoxy carbonyl moiety, respectively. The molecular structure of the complex shows that the molecule is almost coplanar except for one naphthyl ring. The coplanarity of the molecule can be shown by the dihedral angles of 14.06(0.08)° and 23.74(0.08)° formed between the central plane S1A/Cu/Cl/S1B and planes N1A/N2A/C11A/S1A and N1B/N2B/C11B/S1B, respectively. The dihedral angles 71.74(0.02) and 15.56(0.07) between central plane S1A/Cu/Cl/S1B and planes of naphthyl rings (C1A/C2A/C3A/···/C9A/C10A) and (C1B/C2B/C3B/···/C9B/C10B), respectively, suggest that only naphthyl ring A is non-coplanar. In ligand, the thiocarbonyl and carbonyl bond lengths are typical of double bonds, whereas all the C–N bond lengths are shorter than normal C–N bonds (1.48 A°), indicating some degree of electron delocalization (table 2). All the bond lengths and angles are consistent with the related substituted thiocarbamides [16]. No net increase in C–N and C=O bond lengths and slight increase in C=S bond length in case of copper complex indicates coordination through thione sulfur only. The coordination geometry of **1a** is almost trigonal planar as reflected by bond angles S1A–Cu–S1B (119.46)°, S1A–Cu–Cl (121.22)°, and S1B–Cu–Cl (119.29)° [38]. The structure of **1a** is similar to bis(N-(o-methylphenyl)-N′-(ethoxycarbonyl thiourea) copper(I) chloride [38]. A strong intramolecular hydrogen bond interaction is observed between N1/H1 and carbonyl oxygen forming a pseudo-six-membered ring; C12/N2/C11/N1/H1···O1 with non-bonding distance N1···O1, 2.674 Å observed in the ligand remains unaffected in **1a**. This probably prevents carbonyl oxygen from participating in coordination. In the case of complex, an additional intramolecular hydrogen bonding interaction N–H···Cl is observed between chloride (Cl) and N2A/H2A and N2B/H2B, respectively, forming a six-membered ring in each case with non-bonding distances of 3.2145 and 3.2126 Å (table 2). As a consequence of these intense intramolecular interactions, the complex assumes almost coplanar conformation. Weak intermolecular interactions (C–H···O, C–H···Cl, and Cπ···Cπ) stabilize the crystal packing and lead to an infinite chain length along the *c*-axis [figure 2(b)].

3.3. *Geometry optimization of 1 and 1a*

Molecular structures of ligand and complex were optimized at B3LYP/6-311 + G(d,p) level in gaseous phase using coordinates of SCXRD and are shown in figure S2(a) and (b). Point group symmetry of both compounds is C_1. Dipole moment values for the ligand and complex are 3.80 and 0.83 Debye, respectively. The low value for the complex indicates its symmetrical structure. Calculated bond lengths and angles presented in tables 2 and 3 show close resemblance with experimental values.

3.4. *NMR study*

In the ^{1}H NMR spectrum of the complex, the characteristic signal for –CONH at 8.37 ppm in ligand undergoes a downfield shift of ~3.00 ppm following coordination of thione sulfur of ligand to Cu(I). This downfield shift is probably due to intramolecular hydrogen bonding between –CONH and coordinated chloride. This observation infers that the above intramolecular hydrogen bonding remains intact in solution also. The hydrogen-bonded –CSNH ((C=S)–NH···O=C) signal at 11.62 ppm in the ligand remains practically unchanged in the

Table 3.   Selected DFT calculated IR frequencies of ligand and their assignments. Experimental values are given in parenthesis.

Wavenumber/cm^{-1}	Intensity	Assignments
641	74	Op bending of N–H
783(774)	39	Op bending of N–H coupled with C=O op bending
790	75	Op bending of C–H of benzene ring
1056(1034)	191	C–O str coupled with umbrella motion of C–H in terminal methyl group
1175(1199)	150	Ip bending of N–H coupled with C–H ip bending and C–N str
1245(1245)	330	C–O str coupled with N–H and C–H ip bending
1378(1347)	588	C⋯N str
1394(1546)	94	C=C str in Naphthalene coupled with C⋯N str
1540(1534)	589	N–H ip bending coupled with C⋯N str
1594	472	N–H ip bending coupled with C⋯N str
1759(1725)	292	C=O str coupled with N–H ip bending
3057(2960)	32	Sym C–H str in methyl group
3134	14	Asym C–H str in methyl group
3166	11	Asym C–H str in methyl group
3186(3009)	29	C–H str in Naphthyl group
3427(3151)	249	N–H str
3609(3435)	77	N–H str

Table 4.   Selected DFT calculated IR frequencies of complex and their assignments. Experimental values are given in parenthesis.

Wavenumber/cm^{-1}	Intensity	Assignments
500	14	Molecular vibration
713	35	Op bending of N–H
726	26	Op bending of N–H
732(729)	39	Op bending of C–H in Naphthyl group
791(778)	92	Op bending of C–H in Naphthyl group
1064	99	C–O str coupled with ip bending of C–H
1066	62	C–N str coupled with C–O str and ip bending of C–H of Naphthyl group
1070	104	C–O str coupled with C–N str
1209(1178)	103	Rocking of C–H in methyl group
1227	197	C–S str coupled with N–H ip bending
1230(1226)	197	C–S str coupled with N–H ip bending and C–H ip bending
1240(1230)	173	C=C str in Naphthyl group coupled with N–H ip bending
1289	938	C⋯O str
1373	65	Ip bending of C–H in Naphthyl group
1378(1368)	200	C=N str coupled with N–H ip bending
1380	416	C=N str coupled with N–H ip bending
1565(1525)	900	N–H ip bending coupled with C–N str
1574	92	N–H ip bending coupled with C–N str
1583	265	N–H ip bending coupled with C=N str
1591	970	N–H ip bending coupled with C=N str
1751(1746)	637	C=O str coupled with N–H ip bending
1753	94	C=O str coupled with N–H ip bending
3055(2961)	52	Sym C–H str in terminal methyl group
3131	21	Asym C–H str in methyl group
3186(3103)	40	C–H str in Naphthalene
3211	2131	Asym N–H str towards Cl
3254	131	Sym N–H str towards Cl
3383(3169)	330	N–H str
3392	378	N–H str

complex, confirming that carbonyl oxygen does not coordinate. The signals at 180 and 154 ppm in the ^{13}C NMR spectrum of ligand correspond to C=S and C=O carbons, respectively, and appear almost at the same position in the spectrum of **1a**. ^{1}H and ^{13}C NMR spectroscopic details of compounds matched well with related thiourea compounds [38].

3.5. *IR study*

IR spectra of NMCT and its copper complex recorded from 4000 to 400 cm^{-1} are shown in figures S3 and S4 along with the DFT-calculated frequencies (shown by vertical lines). The DFT-calculated vibrational frequencies for the ligand and complex are presented in tables 3 and 4, respectively, along with their assignments. It is clear that theoretical vibrational bands show close proximity to their experimental counterparts. The correlation between calculated and experimental spectra is based on peak intensities and peak frequencies (cm^{-1}). The experimental results are interpreted and rationalized by the theoretical investigations based upon the DFT calculations. Though matching between theoretical and experimental frequencies is good at low wavenumbers, there are deviations at higher wavenumbers due to increase in anharmonicity. To overcome the above problem, scaling factors of 0.977 and 0.945 have been applied between 1500–2800 cm^{-1} and 2800–3650 cm^{-1}, respectively. In ligand, the high energy band at 3435 due to free –NH undergoes a red shift of 250 cm^{-1} in its complex owing to formation of intramolecular hydrogen bonding with chloride (–(C=O) N–H···Cl), whereas the second band at 3151 cm^{-1} due to intramolecularly hydrogen-bonded –NH does not show any shift. A positive shift of 20 cm^{-1} in ν(C–N) and a negative shift of 15 cm^{-1} in ν(C=S) in **1a** when compared to ligand suggests coordination through thione sulfur [15]. A small shift in ν(–C=S) on coordination may be attributed to N–H···O=C and N–H···Cl–Cu intramolecular hydrogen bonding which reduces the delocalization of bonds in thione moiety and consequently increasing its double bond character. The coordination through thione sulfur is further supported by a positive shift of 20 cm^{-1} in ν(C=O). This is consistent with the related thiourea derivatives [15].

3.6. *Electronic study*

Electronic spectra of **1** and **1a** were recorded in dichloromethane and are presented in figure 3(a) and (b), respectively. Absorption spectrum of **1** consists of only one band at λ_{max} 270 nm with tail extending to 350 nm. This band is mainly due to intraligand charge transfer transition with a small contribution from ligand-to-ligand charge transfer transition. Absorption spectrum of complex consists of mainly two bands, one at 300 nm and another at 345 nm, which occur due to interligand charge transfer and metal-to-ligand charge

Table 5. Selected TD-DFT calculated results for the absorption spectrum of ligand at B3LYP/6-311 + G(d,p).

Wavelength/nm	Oscillator strength	Energy/eV	Transitions occurring	Assignment
371	0.0118	3.34	68 → 69	Π(Np)/n(N/S/O) → Π*(Np)/Π*(NCS/COO)
326	0.1603	3.79	67 → 69	Π(Np)/n(N/S) → Π*(Np)/Π*(NCS/COO)
302	0.0158	4.1	68 → 70	Π(Np)/n(N/S/O) → Π*(Np)/Π*(NCS/COO)
287	0.0116	4.31	66 → 69	Π(Np)/n(N/S/O) → Π*(Np)/Π*(NCS/COO)
273	0.0488	4.53	67 → 70	Π(Np)/n(N/S) → Π*(Np)/Π*(NCS/COO)
259	0.0666	4.78	67 → 71	Π(Np)/n(N/S) → Π*(Np)
246	0.0538	5.02	67 → 71	Π(Np)/n(N/S) → Π*(Np)
245	0.1355	5.05	66 → 70	Π(Np)/n(N/S/O) → Π*(Np)/Π*(NCS/COO)

Table 6.   Selected TD-DFT calculated results for the absorption spectrum of complex at B3LYP/6-311 + G(d,p).

Wavelength/nm	Oscillator strength	Energy/eV	Transitions occurring	Assignment
391	0.004	3.17	159 → 160	P(S)/d(Cu)/n(Cl) → π*(Ph/NCS)
381	0.006	3.25	158 → 160	P(S)/d(Cu)/n(Cl) → π*(Ph/NCS)
339	0.0902	3.65	157 → 160	P(S)/d(Cu)/π(Ph) → π*(Ph/NCS)
304	0.1382	4.07	157 → 162	P(S)/d(Cu)/π(Ph) → π*(Ph/COO/NCS)
302	0.0519	4.1	155 → 160	π(Ph)/d(Cu)/n(Cl) → π*(Ph/NCS)
297	0.0276	4.17	155 → 161	π(Ph)/d(Cu)/n(Cl) → π*(Ph/COO/NCS)
289	0.0272	4.28	157 → 163	P(S)/d(Cu)π(Ph) → π*(COO/NCS)
262	0.0238	4.72	152 → 160	P(S)/d(Cu)/π(Ph)/n(Cl) → π*(Ph/NCS)
233	0.0738	5.3	152 → 163	P(S)/d(Cu)/π(Ph)/n(Cl) → π*(COO/NCS)
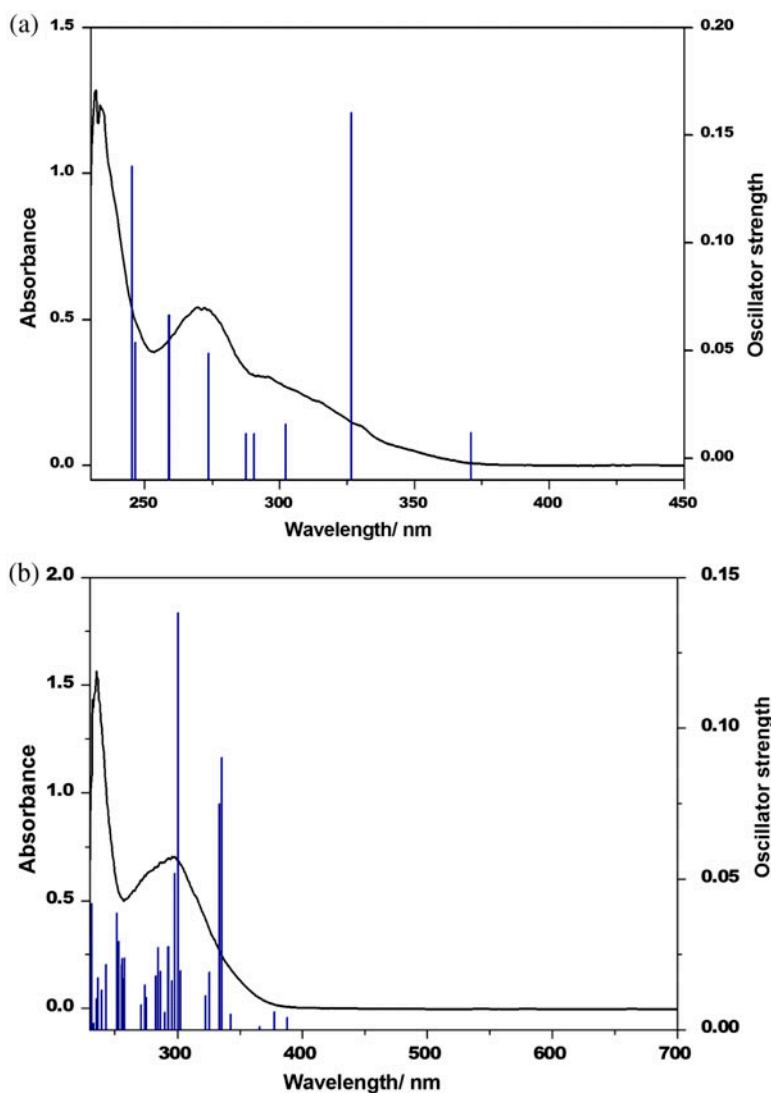
Figure 3.   Experimental (curved lines) and TD-DFT calculated (vertical lines) absorption spectra in dichloromethane (a) NMCT (**1**) and (b) (NMCT)₂CuCl (**1a**).
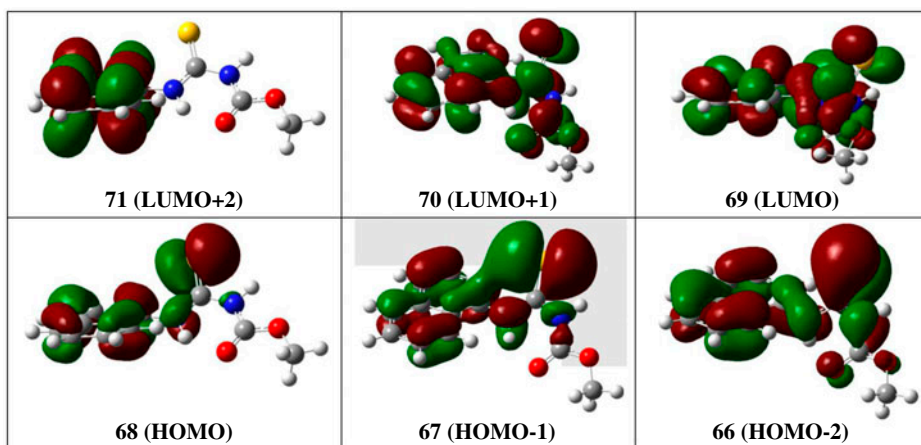
Figure 4.   The FMO pictures of ligand involved in electronic transitions.

transfer transitions, respectively. To get deeper insight into electronic transitions involved at different wavelengths, TD-DFT calculations are tabulated in tables 5 and 6, respectively. In both cases, the experimentally observed bands match with those obtained from TD-DFT calculations (figures 3 and 4). The Frontier molecular orbital (FMO) pictures of some important transitions for ligand and complex are shown in figures 4 and 5, respectively.
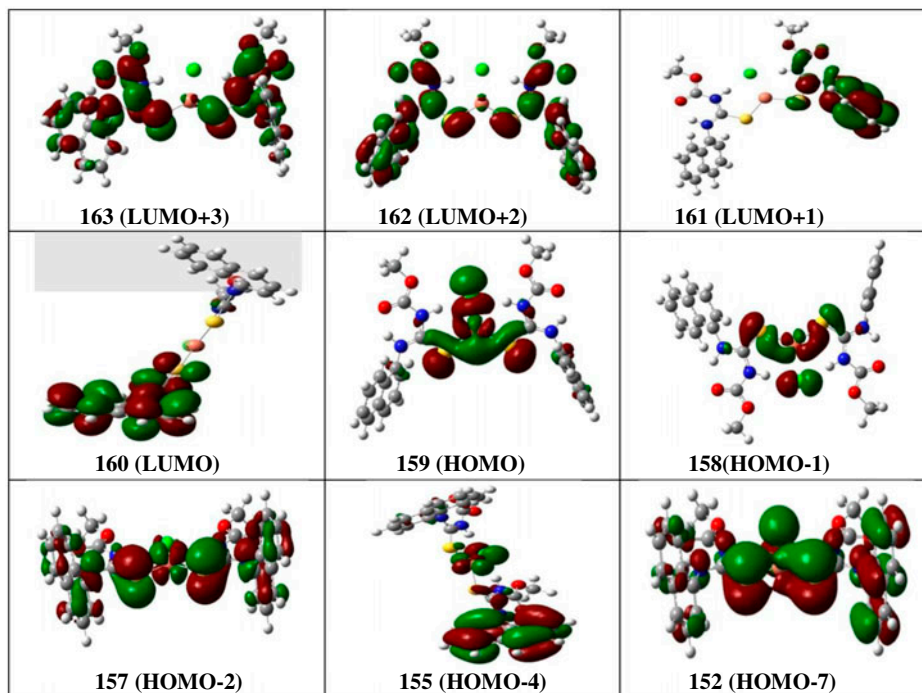

Figure 5.   The FMO pictures of complex involved in electronic transitions.

Table 7. IC$_{50}$ values (μM) for the compounds and their Cu complexes against two human cervical cancer cell lines (2008 and C13*) and three human ovarian carcinoma cell lines (A2780, A2780/CP and IGROV-1).

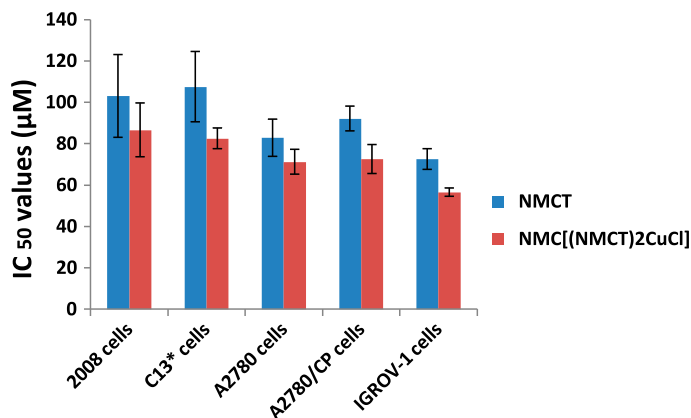| Compounds	2008 cells	C13* cells	A2780 cells	A2780/CP cells	IGROV-1 cells
NMCT (**1**)	103 ± 20	107 ± 17	83 ± 9	92 ± 6	72 ± 5
(NMCT)$_2$CuCl (**1a**)	9 ± 13	82 ± 5	71 ± 6	72 ± 7	56 ± 2
Cisplatin	1.9 ± 0.5	19 ± 1	2.1 ± 0.4	20 ± 2	1.6 ± 0.2
5-FU	4.1 ± 0.3	8.5 ± 0.5	5.5 ± 0.3	12.8 ± 0.5	5.1 ± 0.2

Figure 6.   Comparative cytotoxicity of **1** and **1a**.

3.7. *Cytotoxicity study*

1 and **1a** have been tested for their *in vitro* cytotoxicity against two human cervical carcinoma (2008 and C13*) and three ovarian carcinoma (A2780, A2780/CP, and IGROV-1) cell lines in which C13* and A2780/CP are cisplatin resistant. The IC$_{50}$ values (the concentration which produces 50% growth inhibition of cell lines) for the compounds along with two standard drugs are given in table 7. Both compounds exhibited moderate activity against all the cancer cell lines, but the lowest IC$_{50}$ values were observed against IGROV-1 cells. The inhibitory activity of copper complex was stronger than the ligand (figure 6). The better activity of copper complex may be related to the redox behavior of copper, which is believed to initiate the production of highly reactive hydroxyl radicals responsible for damaging biomolecular species like lipid, protein, and DNA [49–51].

4. Conclusion

In **1a,** the ligand binds through thione sulfur only. The non-participation of carbonyl oxygen is probably due to strong intramolecular hydrogen bonding with –NH. The single-crystal study reveals an almost symmetrical trigonal planar structure of the complex. FT-IR, ^{1}H NMR, ^{13}C NMR, and UV–visible spectral studies also support the above structure. The detailed assignment of vibrational frequencies and electronic transitions were done by DFT studies. The cytotoxicity screening results against five cancer cell lines show that copper complex exhibited better activity than ligand.

Supplementary material

CCDC 1017873 and 945655 contain the supplementary crystallographic data for NMCT (**1**) and its copper complex **1a**. These data can be obtained free of charge at http://www.ccdc. cam.ac.uk/data_request/cif, by e-mailing deposit@ccdc.cam.ac.uk or by contacting the Cambridge Crystallographic Data Center, 12 Union Road, Cambridge CB2 1EZ, UK; Fax: +44 1223 336033.

Acknowledgements

References

[1] N. Selvakumaran, A. Pratheepkumar, S.W. Ng, E.R.T. Tiekink, R. Karvembu. *Inorg. Chim. Acta*, **404**, 82 (2013).
[2] N. Selvakumaran, S.W. Ng, E.R.T. Tiekink, R. Karvembu. *Inorg. Chim. Acta*, **376**, 278 (2011).
[3] Z. Weiqun, Y. Wen, X.L. Liqun. *J. Inorg. Biochem.*, **99**, 1314 (2005).
[4] A.M. Plutín, R. Mocelo, A. Alvarez, R. Ramos, E.E. Castellano, M.R. Cominetti, A.E. Graminha, A.G. Ferreira, A.A. Batista. *J. Inorg. Biochem.*, **134**, 76 (2014).
[5] B. Lal, A. Badshah, A.A. Altaf, M.N. Tahir, S. Ullah, F. Huq. *Dalton Trans.*, **41**, 14643 (2012).
[6] C. Sacht, M.S. Datt, S. Otto, A. Roodt. *Dalton Trans.*, 4579 (2000).
[7] K.G. Daniel, D. Chen, S. Orlu, Q.C. Cui, F.R. Miller, Q.P. Dou. *Breast Cancer Res.*, **7**, R897 (2005).
[8] A.N. Mautjana, J.D.S. Miller, A. Gie, S.A. Bourne, K.R. Koch. *Dalton Trans.*, 1952 (2003).
[9] N.H. Huy, U. Abram. *Inorg. Chem.*, **46**, 5310 (2007).
[10] D.J. Che, X.L. Yao, G. Li, Y.H. Li. *Dalton Trans.*, 1853 (1998).
[11] D.J. Che, G. Li, X.L. Yao. *Dalton Trans.*, 2683 (1999).
[12] A. Laguna, P.G. Jones. *Inorg. Chim. Acta*, **324**, 319 (2001).
[13] N.H. Huy, U. Abram. *Inorg. Chem.*, **46**, 5310 (2007).
[14] N. Gunasekaran, P. Ramesh, M.N.G. Ponnuswamy, R. Karvembu. *Dalton Trans.*, **40**, 12519 (2011).
[15] J. Duque, O. Estévez-Hernández, E. Reguera, J. Ellena, R.S. Corrêa. *J. Coord. Chem.*, **62**, 2804 (2009).
[16] X. Shen, X. Shi, B. Kang, Y. Liu, Y. Tong, H. Jiang, K. Chen. *Polyhedron*, **17**, 4049 (1998).
[17] H.Y. Yuen, W. Henderson, A.G. Oliver. *Inorg. Chim. Acta*, **368**, 1 (2011).
[18] M.G. Babashkina, D.A. Safin, M. Bolte, A. Klein. *Inorg. Chem. Commun.*, **12**, 678 (2009).
[19] T.S. Smith, W. Henderson, B.K. Nicholson. *Inorg. Chim. Acta*, **408**, 27 (2013).
[20] S. Saeed, N. Rashid, P.G. Jones, M. Ali, R. Hussain. *Eur. J. Med. Chem.*, **45**, 1323 (2010).
[21] A.A. Isab, S. Nawaz, M. Saleem, M. Altaf, M. Monim-al-Mehboob, A. Ahmad, H.S. Evan. *Polyhedron*, **29**, 1251 (2010).
[22] A. Saeed, U. Shaheen, A. Hameed, S.Z.H. Naqvi. *J. Fluorine Chem.*, **130**, 1028 (2009).
[23] M.K. Rauf, I. Din, A. Badshah, M. Gielen, M. Ebishara, D. Vos, S. Ahmed. *J. Inorg. Biochem.*, **103**, 1135 (2009).
[24] V.R. Solomon, W. Haq, M. Smilkstein, K. Srivastava, S.K. Puri, S.B. Katti. *Eur. J. Med. Chem.*, **45**, 4990 (2010).
[25] W. Yang, H. Liu, M. Li, F. Wang, W. Zhou, J. Fan. *J. Inorg. Biochem.*, **116**, 97 (2012).
[26] H. Pérez, B. O'Reilly, A.M. Plutín, R. Martínez, R. Durán, I.G. Collado, Y.P. Mascarenhas. *J. Coord. Chem.*, **64**, 2890 (2011).
[27] M. Domínguez, E. Anticó, L. Beyer, A. Aguirre, S. García-Granda, V. Salvadó. *Polyhedron*, **21**, 1429 (2002).
[28] V. Carcu, M. Ilie, M. Ilis, F. Dumitrascu, I. Neagoe, S. Pasculescu. *Polyhedron*, **28**, 3739 (2009).
[29] M.M. Habtu, S.A. Bourne, K.R. Koch, R.C. Luckay. *New J. Chem.*, **30**, 1155 (2006).
[30] J.C. Bruce, N. Revaprasadu, K.R. Koch. *New J. Chem.*, **31**, 1647 (2007).
[31] N. Gunasekaran, P. Jerome, S.W. Ng, E.R.T. Tiekink, R. Karvembu. *J. Mol. Catal. A: Chem.*, **353**, 156 (2012).
[32] J.P. Holland, J.C. Green. *J. Comput. Chem.*, **31**, 1008 (2010).
[33] S. Triki, C.J. Gómez-García, E. Ruiz, J. Sala-Pala. *Inorg. Chem.*, **44**, 5501 (2005).

[34] A. Ghosh, I. Halvorsen, H.J. Nilsen, E. Steene, T. Wondimagegn, R. Lie, E. van Caemelbecke, N. Guo, Z. Ou, K.M. Kadish. *J. Phys. Chem. B*, **105**, 8120 (2001).

[35] P.J. Blower, T.C. Castle, A.R. Cowley, J.R. Dilworth, P.S. Donnelly, E. Labisbal, F.E. Sowrey, S.J. Teat, M.J. Went. *Dalton Trans.*, **23**, 4416 (2003).

[36] S. Demeshko, S. Dechert, F. Meyer. *J. Am. Chem. Soc.*, **126**, 4508 (2004).

[37] G.A. Bain, J.F. Berry. *J. Chem. Educ.*, **85**, 532 (2008).

[38] L. Xian, T.-B. Wei, Y.-M. Zhang. *J. Coord. Chem.*, **57**, 453 (2004).

[39] G.M. Sheldrick. *Acta Crystallogr. Sect. A*, , **64**, 112 (2008).

[40] M.N. Burnett, C.K. Johnson. *Report ORNL-6895*, Oak Ridge National Laboratory, Oak Ridge, TN (1996).

[41] C.F. Macrae, I.J. Bruno, J.A. Chisholm, P.R. Edgington, P. Mc Cabe, E. Pidcock, L. Rodriguez-Monge, R. Taylor. *J. Appl. Cryst.*, **41**, 466 (2008).

[42] M.J. Frisch, G.W. Trucks, H.B. Schlegel, G.E. Scuseria, M.A. Robb, J.R. Cheeseman, J.A. Montgomery Jr. T. Vreven, K.N. Kudin, J.C. Burant, J.M. Millam, S.S. Iyengar, J. Tomasi, V. Barone, B. Mennucci, M. Cossi, G. Scalmani, N. Rega, G.A. Petersson, H. Nakatsuji, M. Hada, M. Ehara, K. Toyota, R. Fukuda, J. Hasegawa, M. Ishida, T. Nakajima, Y. Honda, O. Kitao, H. Nakai, M. Klene, X. Li, J.E. Knox, H.P. Hratchian, J.B. Cross, V. Bakken, C. Adamo, J. Jaramillo, R. Gomperts, R.E. Stratmann, O. Yazyev, A.J. Austin, R. Cammi, C. Pomelli, J.W. Ochterski, P.Y. Ayala, K. Morokuma, G.A. Voth, P. Salvador, J.J. Dannenberg, V.G. Zakrzewski, S. Dapprich, A.D. Daniels, M.C. Strain, O. Farkas, D.K. Malick, A.D. Rabuck, K. Raghavachari, J.B. Foresman, J.V. Ortiz, Q. Cui, A.G. Baboul, S. Clifford, J. Cioslowski, B.B. Stefanov, G. Liu, A. Liashenko, P. Piskorz, I. Komaromi, R.L. Martin, D.J. Fox, T. Keith, M.A. Al-Laham, C.Y. Peng, A. Nanayakkara, M. Challacombe, P.M.W. Gill, B. Johnson, W. Chen, M.W. Wong, C. Gonzalez, J.A. Pople, GAUSSIAN 03, REVISION D.02, Gaussian, Inc., Wallingford, CT (2004).

[43] W. Kohn, L. Sham. *J. Phys. Rev. B*, **140**, 1133 (1965).

[44] C. Lee, W. Yang, R.G. Parr. *Phys. Rev. B*, **37**, 785 (1988).

[45] A.D. Becke. *J. Chem. Phys.*, **98**, 5648 (1993).

[46] C. Korch, M.A. Spillman, T.A. Jackson, B.M. Jacobsen, S.K. Murphy, B.A. Lessey, V.C. Jordan, A.P. Bradford. *Gynecol. Oncol.*, **127**, 241 (2012).

[47] P.A. Andrews, J.A. Jones. *Cancer Commun.*, **3**, 1 (1991).

[48] T. Mosmann. *J. Immunol. Methods*, **16**, 55 (1983).

[49] K. Wong, A.R. Morgan, W. Parachych. *Can. J. Biochem.*, **52**, 950 (2001).

[50] M.T. Yahaya, T.M. Straub. International Copper Research Association 2001 Project 48.

[51] U.G. Lopes, P. Erhardt, R. Yao, G.M. Cooper. *J. Biol. Chem.*, **272**, 12893 (1997).